Crystallization Times of As-deposited and Melt-quenched Amorphous Phase Change Materials

Simone Raoux[1], Robert Shelby[1], Becky Munoz[2], Martina Hitzbleck[3], Daniel Krebs[3], Martin Salinga[3], Michael Woda[3], Michael Austgen[3], Kyung-Min Chung[3] and Matthias Wuttig[3]
[1]IBM Macronix PCRAM Joint Project, IBM Almaden Research Center, 650 Harry Road, San Jose, CA 95120
[2]Boise State University, Department of Materials Science and Engineering, Boise, ID 83725
[3]1. Physikalisches Institut 1A, RWTH Aachen, Aachen, Germany

ABSTRACT

The crystallization time of various phase change materials including $Ge_{15}Sb_{85}$, Ag- and In-doped Sb_2Te (AIST), $Ge_3Sb_6Te_5$ and $Ge_2Sb_2Te_5$ was studied using static laser testers. It was found that there is a large difference in crystallization time between these materials. In addition, for some materials there is a large difference (up to almost three orders of magnitude) between the crystallization time of as-deposited, amorphous, and melt-quenched, amorphous material. The crystallization time of as-deposited materials ranges from about 150 ns for $Ge_2Sb_2Te_5$ to tens of μs for AIST, while the crystallization time for melt-quenched, amorphous materials varies between 20 ns for $Ge_{15}Sb_{85}$ and about 1μs for $Ge_3Sb_6Te_5$.

Key words: crystallization time, as-deposited, melt-quenched, amorphous

1. INTRODUCTION

The crystallization time of phase change materials is one of the most important properties as it influences the data rate for both, optical storage and Phase Change Random Access Memory (PCRAM) devices. Even though phase change technology was invented more than 40 years ago [1], only the discovery of fast crystallizing materials, in particular the materials along the pseudo-binary line between GeTe and Sb_2Te_3 [2], enabled the whole development of phase change optical storage technology. Crystallization occurs by the formation of crystalline nuclei and their subsequent growth, and depending on the nature of the phase change material one or the other mechanism can dominate the crystallization time. In nucleation-dominated materials the crystallization proceeds primarily by the formation of new nuclei while their subsequent growth is relatively slow. The crystallization time dominated by the formation of new nuclei depends on the order present in the amorphous phase such as the degree of medium range order and the existence of very small crystalline nuclei in the amorphous phase [3]. In growth-dominated materials incubation times (times to form the first nuclei) can be long, but as soon as they have formed the crystallization proceeds by growth from the amorphous-crystalline interface typically with great speed. The presence of such amorphous-crystalline interfaces, as they probably exist in all optical storage media and PCRAM device variations, makes these materials useful for technological applications. The crystallization time is not exclusively an inherent property of the phase change material itself. The interface between the phase change material and its surrounding also plays a role for the crystallization time, and depending on the surrounding material can be increased or reduced [4]. The importance of interfaces is also evident from the fact that the crystallization and incubation times depend on the thickness of the phase change material [5-7]. A reduction in films thickness was found to decrease (for growth-dominated Ag-In-Sb-Te materials) or increase (for nucleation-dominated Ge-Sb-Te materials) the crystallization time [5]. In another case a minimum in the crystallization time was found at an optimized film thickness [6]. An increase in incubation times by orders of magnitude was observed when the film thicknesses were reduced to the few nanometer range for $Ge_2Sb_2Te_5$ [7].

This paper describes measurements of the crystallization time of various phase change materials including nucleation- and growth-dominated materials from the Ge-Sb-Te family and growth-dominated materials from the Ag-In-Sb-Te

family and the Ge-Sb system. The crystallization times of as-deposited, amorphous and melt-quenched, amorphous materials are compared.

2. EXPERIMENTS

Thin films of phase change material (30 – 70 nm thick) were deposited on glass or Si wafers with a thin (50 nm) Al_2O_3 heat barrier layer by magnetron sputtering using alloy targets. Laser testing was performed on two different static laser testers. The first tester is described in detail in [8] and the second in [9]. The first laser set-up consisted of only one pulsed laser which was used to measure the reflectivity before and after exposure to a laser pulse that induced phase transitions. This tester cannot provide information about the change in reflectivity during the phase-change-inducing pulse. Nevertheless, it is an easy tool to screen new phase change materials quickly. The second laser tester consisted of a high power, pulsed laser with variable laser pulse duration and power used to induce phase transitions in the sample, and a low power, cw laser that constantly monitored the reflectivity of the sample.

Several types of laser experiments were performed.

Single-pulse experiments: The simplest experiment is the exposure of an as-deposited, amorphous film to laser pulses of variable power and duration and the detection of which powers and durations cause crystallization. Crystallization in phase change materials is typically connected with an increase in reflectivity, but one needs to perform a "sanity check", using for example atomic force microscopy (AFM), to confirm the crystallization because other effects such as changes in the topography of the sample can also lead to changes in reflectivity but without crystallization. From measurements of the resistivity as a function of temperature the crystallization temperature of the materials was determined. Samples were annealed at temperatures 20 – 50 ºC above the crystallization temperature for 10 min in a furnace in a nitrogen or argon atmosphere to crystallize them. Single-pulse experiments were then performed to attempt melt-quenching of the material connected with a decrease in reflectivity.

Post-pulse experiments: In the melt-quenching, single-pulse experiment described above it can be difficult to distinguish between reduction in reflectivity due to melt-quenching and due to ablation of the material. One can do this by annealing the sample again over its crystallization temperature and subsequently investigating the sample using either a high resolution optical microscope or AFM. Melt-quenched laser spots will have disappeared (re-crystallized in the crystalline matrix) but ablated will not. One can also use AFM to image the original exposed sample where melt-quenching leads to a small increase in height of a few nm, but ablation to a very large change in topography. A more elegant way to measure melt-quenching properties is a post-pulse experiment. Here a crystalline film is exposed first to a pulse of variable power and duration to melt-quench the material, reflectivity is measured, the sample is exposed to a second pulse of fixed power and duration (selected from the single-pulse experiment on the as deposited films in the duration and power range were reliable crystallization occurs), and reflectivity is measured again. In the area where the reflectivity is reduced after the first pulse and restored to the value before the experiment melt-quenching and re-crystallization has occurred. In the area where the reflectivity is reduced after the first and second pulse ablation has occurred.

Pre-pulse experiments: Pre-pulse experiments are designed to measure the crystallization time that is relevant to technological devices (optical discs and PCRAM), even though, as mentioned in the introduction, the ultimate measurement needs to be performed using the actual device because the crystallization time depends on so many parameters. It is a good method however to screen materials quickly by comparing crystallization times of various materials with identical thickness on identical substrates and (optionally) with identical capping layers. Here a pre-pulse with fixed duration and power (selected from the post-pulse experiment in the range were reliable melt-quenching without ablation occurs) is used to make a melt-quenched spot of a fixed size in a crystalline film, and a second pulse with variable duration and power is used to attempt re-crystallization. This is the relevant time for technological applications since this condition comes closest to disc or PCRAM switching conditions. In addition, this experiment can also be an easy and fast method to determine the crystallization mechanism of a new material. If the re-crystallization time depends on the size of the amorphous mark, the material is growth dominated, if not it is nucleation dominated.

3. RESULTS & DISCUSSION

$Ge_{15}Sb_{85}$ is an interesting phase change material because it has a relatively high crystallization temperature (about 250ºC [10]) indicative of a good archival lifetime and thermal stability. Thin films (50 nm thick, composition Ge:Sb=14.3 at% : 85.7 at% with an accuracy of ± 0.5 at% determined by Rutherford Backscattering Spectrometry - RBS) were first studied on glass substrates using the first tester. Figure 1 shows optical microscope images of an as-deposited (Fig.1a) and crystalline film (Fig. 1b) after a single-pulse experiment with pulse duration varying from 5 ns to 10 µs (increased on an exponential scale) in horizontal direction and laser power increased from 5 mW to 35 mW (also increased on an exponential scale) in vertical direction.

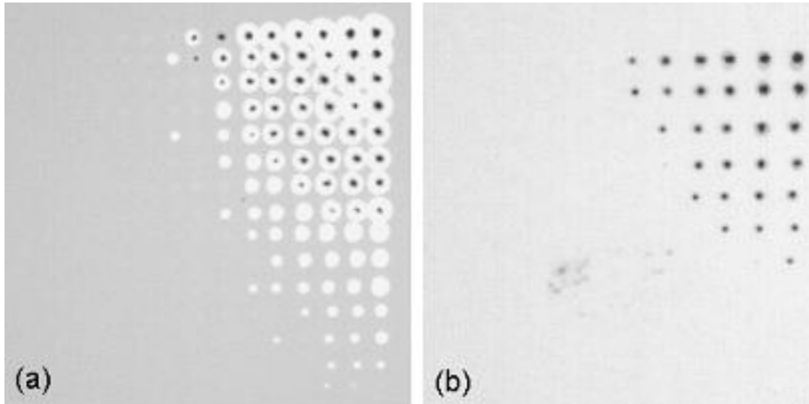

Fig. 1: Optical microscope images of as-deposited (a) and crystalline (b) $Ge_{15}Sb_{85}$ after a single-pulse experiment with pulse duration varying from 5 ns to 10 µs (increased on an exponential scale) in horizontal direction and laser power increased from 5 mW to 35 mW (also increased on an exponential scale) in vertical direction. Images have been contrast-enhanced for better visibility, the increase in reflectivity for as-deposited $Ge_{15}Sb_{85}$ was about 15%. Spot-to-spot distance 5 µm.

One can see in Fig. 1a crystallized (bright) spots, the very first crystallized spots appear after 130 ns long pulses, reliable crystallization occurs after 350 ns long pulses. For high power pulses ablation is observed in the right upper corner of the exposed area. Such an optical image is very informative, because the change in reflectivity was close to zero in some area where the increase in reflectivity due to crystallization and decrease in reflectivity due to ablation in the center of the spot just cancelled each other. The duration and power limits for which crystallization occurs are not well defined and crystallization appears somewhat random in the borderline area. Even spots can be found that show ablation in the middle but no crystallization. This is an indication of a growth dominated material. There is typically only one (and sometimes no) nucleation site per spot from which the crystal grows. In Fig. 1b a reduction in reflectivity is observed, but this is not connected to melt-quenching. The dark areas are ablated because they did not disappear upon annealing of the sample. The crystallization of melt-quenched $Ge_{15}Sb_{85}$ happens so fast that the heat cannot be conducted away fast enough after melting to quench the material in the amorphous phase. It crystallizes during cooling. In order to measure crystallization time of melt-quenched $Ge_{15}Sb_{85}$ the material was deposited on a Si waver coated with a thin (50nm) Al_2O_3 heat barrier. Figure 2 shows the change in reflectivity for a 30 nm thick crystalline $Ge_{15}Sb_{85}$ film after a single-pulse experiment (second laser tester used).

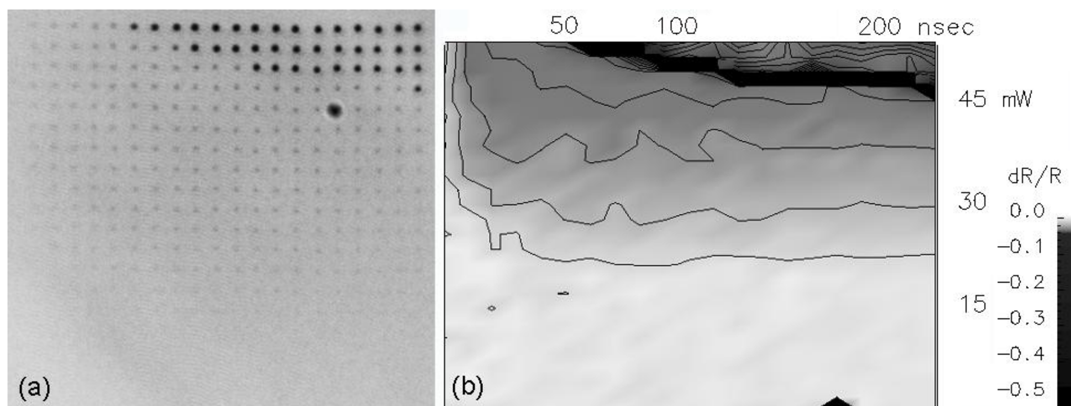

Fig. 2: (a) Optical microscope image (contrast enhanced) and (b) relative change in reflectivity after single pulse experiment with duration from 10 – 200 ns (horizontal, increased linearly) and power from 2.5 - 50 mW (vertical, increased linearly).

The relative change in reflectivity is defined as $dR/R = (R_{after} - R_{before}) / R_{before}$, where R_{before} and R_{after} are the reflectivities before and after the variable laser pulse. Here two different shades of darker spots are observed in the optical image, a small reduction in reflectivity corresponding to melt-quenching, and a large one due to ablation. It can be seen that the melt-quenching is very fast, the shortest laser pulse of 10 ns already leads to melt-quenching. Figure 3 compares the crystallization times of as-deposited and re-crystallization time of melt-quenched $Ge_{15}Sb_{85}$.

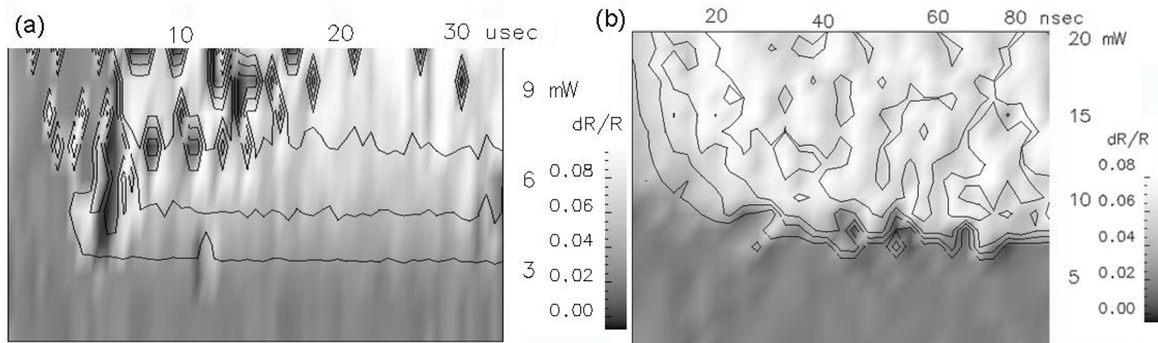

Fig. 3: (a) – dR/R in single pulse experiment for as-deposited, amorphous $Ge_{15}Sb_{85}$. (b) – pre-pulse experiment (pre-pulse 50 ns, 40 mW) on crystalline $Ge_{15}Sb_{85}$.

Figure 3a shows the change in reflectivity in a single-pulse experiment on as deposited material, whereas Fig. 3b shows a pre-pulse experiment on a crystalline film with a melt-quenching pre-pulse of 50 ns and 40 mW. Figure 3a indicates two kinds of crystallization behavior (also visible in Fig. 1). For low power pulses the material crystallizes reliably for pulses longer than a certain time (about 5µs). AFM images show crystalline spots that are much smaller than the laser spot diameter. For higher powers the crystallization occurs more randomly and the same laser power and duration will sometimes create a crystalline mark and sometimes not. This can be explained as follows. There is an optimum temperature where crystallization is fastest and nucleation rate is the highest which can be shown in the so-called time-temperature-transformation diagram [11]. The temperature dependency of the steady-state homogeneous nucleation rate is an extremely strong function of the temperature below this optimum and drops by more than 20 orders of magnitude over a small temperature range [12]. So when the laser power and duration is just sufficient to reach this optimum temperature in the middle of the spot, crystallization starts in the middle of the spot and is very reproducible. At higher powers the temperature in the spot is higher and the nucleation rate is reduced, but with a much weaker temperature dependence [12]. Crystallization starts now with a reduced probability. Figure 4 illustrates this.

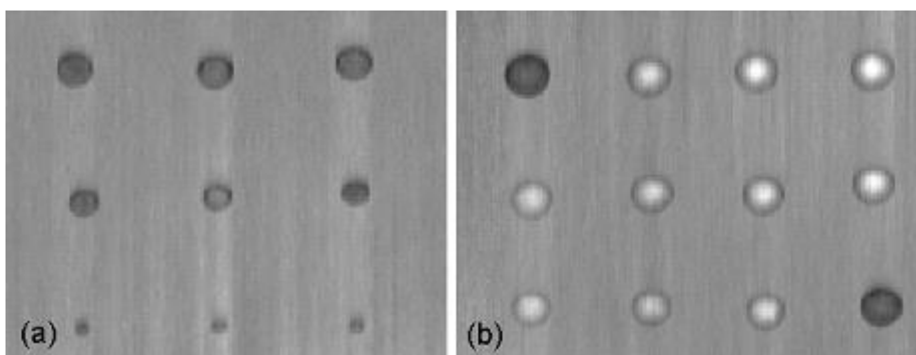

Fig. 4: (a) – AFM image of crystalline spots in as-deposited amorphous $Ge_{15}Sb_{85}$ in the low power region around 4 mW, 15 µs. (b) – AFM image in the high power region around 9 mW, 5 µs. Images taken on the sample shown in Fig. 3a. Spot-to-spot distance 2.5µm.

While the lower laser power leads to reproducible crystallization starting in the center of the pulse, higher laser power leads to more random crystallization with sometimes ablation occurring in the center of the spot. The difference in crystallization times between Figs. 1a and 3a can be explained by the fact that the glass substrate leads to a much slower cooling of the heated area so that after a short laser pulse the sample will still be at elevated temperature for a substantial amount of time during which crystallization can occur. A simulation of the temperature in the laser spot as

a function of laser pulse duration and substrate (using the COMSOL Multiphysics finite element code [13]) showed that for glass substrates the heating and cooling time constants are in the hundreds of ns range. So when the laser pulse was shorter than this time it's duration is not an appropriate measure of the crystallization time since crystallization can occur during cooling long after the laser pulse and the crystallization time can be longer than the laser pulse. For phase change films on 50 nm Al_2O_3 on Si the heating and cooling time constants were found to be about 10 ns, so here the laser duration is the upper limit for the crystallization time for pulses longer than 10 ns. In addition, the laser spots for the first tester were larger (the largest crystalline spots are about 5 μm in Fig. 1a and 1 μm in Fig. 4b), so the chance of a nucleation event in the spot is larger for the first tester.

The really important crystallization time is obtained from Fig. 3b. The re-crystallization of melt-quenched $Ge_{15}Sb_{85}$ occurs in a few nanoseconds, at least 2 orders of magnitude faster than crystallization of as-deposited material. This is the reason why very fast switching (fastest for 4 ns pulses) was demonstrated in actual PCRAM devices using $Ge_{15}Sb_{85}$ [14].

AgIn-Sb_2Te_3 (AIST) is a material that is used in optical storage. Thin films with a composition of Ag:In:Sb:Te = 7 : 11 : 48 : 34 (in at%) with an accuracy of ! 5 at% determined by RBS (Ag:In:(Sb+Te) ratios) and particle induce x-ray emission (Sb:Te ratio) were deposited on 50 nm Al_2O_3 on Si. A single-pulse experiment is shown in Fig. 5 for a 50 nm thick film using the second laser tester.

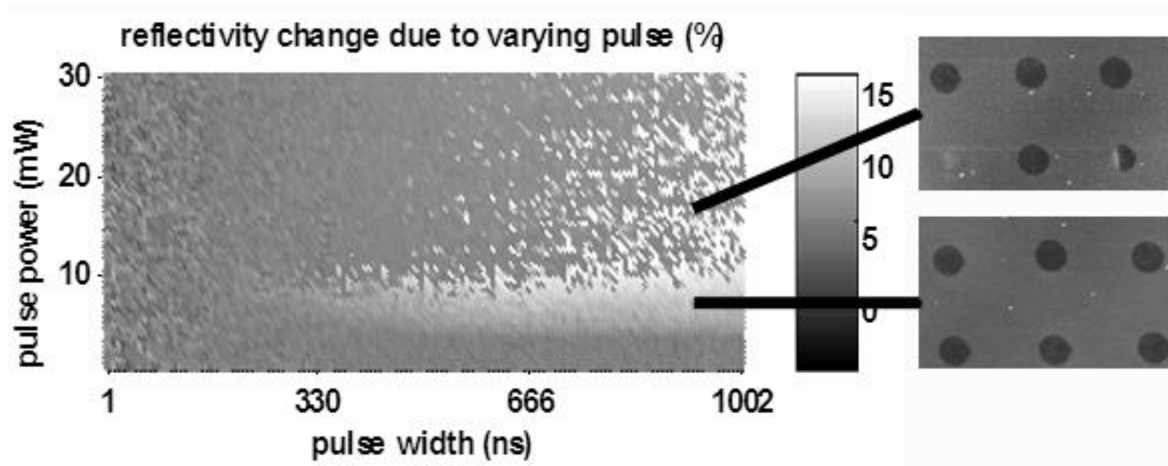

Fig. 5: Single pulse experiment on as deposited AIST and AFM images in two selected areas.

This is a very fine matrix with many laser spots, every pixel on the left side is one laser spot. A similar crystallization behavior to $Ge_{15}Sb_{85}$ was found, reproducible crystallization starting in the middle of the spot for low power, and more random crystallization, sometimes starting at the spot edge, with longer incubation times for higher power. AIST is also a growth dominated material. Figure 6 shows experiments performed on a 50 nm AIST film on a glass substrate using the first tester. The crystallization time of as deposited AIST on glass as determined by a single-pulse experiment was very long, several μs in the higher power range above 10 mW, and a random crystallization probability similar to Fig.5 was found.

Figure 6a shows AFM and optical (Fig. 6b) images of melt-quenched dots in a crystalline film. Here the laser pulse duration was increased from left to right from 100 to 150 ns and the power increased from bottom to top from 28 to 35 mW. Melt-quenched marks of variable size are produced and the top right laser spot shows ablation. The melt-quenched mark is higher than the surrounding crystalline area in the AFM image because the amorphous phase has a lower mass density, but it appears as a dark spot in the optical image because it has lower reflectivity. The melt-quenched mark size was measured as a function of laser duration for a 35 mW laser spot, it increased from 200 nm for 40 ns long pulses to 1000 nm for 150 ns long pulses. Pre-pulse experiments were performed with variable duration of the pre-pulse from 50 ns, 35 mW pulses that produced a 300 nm diameter melt-quenched mark, to 110 ns, 35 mW

pulses that produced a 800 nm diameter melt-quenched mark. Figure 6c shows optical image of the 110 ns, 35 mW pre-pulse experiment.

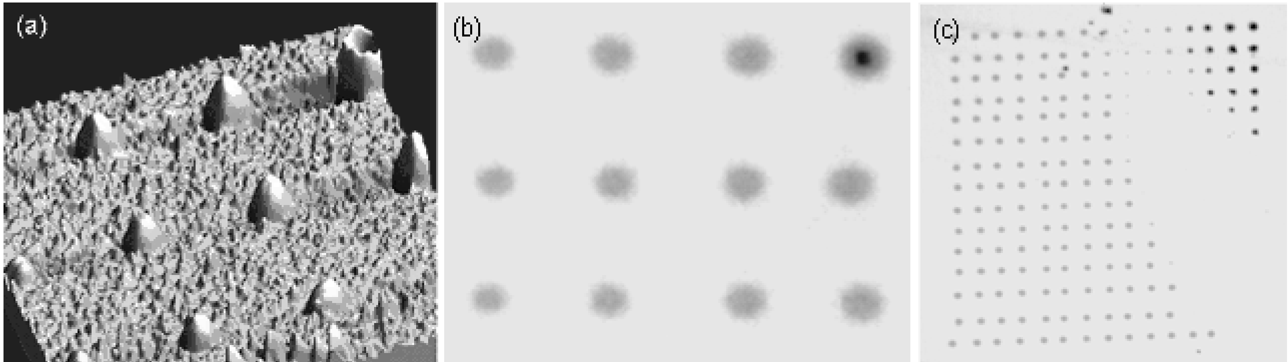

Fig. 6: (a) – AFM image of melt-quenched dots that are shown in the optical image (b). (c) – pre-pulse experiment on AIST with a 110 ns, 35 mW pre-pulse for melt-quenching and subsequent variable pulse ranging from 4 ns to 10 μs (horizontally) and 5 mW to 50 mW vertically.

The duration and power of the second pulse varied between 4 ns and 10 μs (exponential increase) and 6 – 14 mW (exponential increase). On the left side of Fig. 6c identical melt-quenched marks are visible. On the right side an area does not show any contrast. This is the area where re-crystallization of the melt-quenched mark by the second pulse was successful. The fastest re-crystallization for this experiment was 600 ns. On the top right side of Fig. 6c the second pulse led to ablation. The same pre-pulse experiment for pre-pulses of shorter duration (50 ns, smaller mark) required only 200 ns for re-crystallization. The dependency of the re-crystallization time on the size of the amorphous mark indicates that AIST is a growth-dominated material. The fastest re-crystallization time (the relevant time for application) was again much shorter (200 ns) than the crystallization time of as-deposited AIST (in the 1-10 μs range). From the re-crystallization time and the spot diameter the speed of the crystal growth front can be estimated to be in the 0.4 - 0.8 m/s range. This is an averaged value over the different temperatures that exist at various times and locations inside the laser spot. The crystal growth velocity is an exponential function of the temperature [15].

$Ge_3Sb_6Te_5$ is another variation of the Ge-Sb-Te based phase change materials. It is an interesting material because it has a higher crystallization temperature (around 210ºC) than the more commonly used $Ge_2Sb_2Te_5$ (around 150ºC [16]). A higher crystallization temperature can be beneficial for data retention in optical discs and PCRAM applications. Figure 7a shows the change in reflectivity as a function of laser power and duration (first tester used) and the optical image (inset) of an as-deposited, amorphous $Ge_3Sb_6Te_5$ film (70 nm thick, on glass).

The crystallization time for the amorphous film is about 1 μs, and the maximum change in reflectivity is rather high, around 30%. Another sample was annealed and the diameter of melt-quenched dots was determined for 30 mW laser pulses. The spot size varied from 200 nm diameter for 20 ns pulses to 1100 nm diameter for 150 ns. A pre-pulse experiment is shown in Fig. 7b for crystalline $Ge_3Sb_6Te_5$ using a 50 ns, 30 mW pre-pulse. It can be seen that re-crystallization occurs after about 1 μs also, for this material the re-crystallization is not faster than the as-deposited material. Further experiments on the same samples were performed using the second tester. Pre-pulse experiments using variable pre-pulse duration were applied to measure re-crystallization times and compare them to the crystallization time of the as-deposited $Ge_3Sb_6Te_5$. Figure 8a shows the results compared to the same experiment on the more commonly used $Ge_2Sb_2Te_5$ (50 nm deposited on 30 nm Al_2O_3 on Si, second tester) shown in Fig. 8b. As a measure of crystal fraction, dR/R was averaged over the laser power range where the fastest (re-)crystallization was observed (4 – 5 mW for $Ge_3Sb_6Te_5$, 10 – 12 mW for $Ge_2Sb_2Te_5$) and normalized to the dR/R at the longest variable pulse length where the reflectivity did not change anymore with increasing pulse length. The two materials show very different behaviors. While for $Ge_3Sb_6Te_5$ as-deposited and melt-quenched crystallization times are similar (and this is the only material studied here where this is the case), for $Ge_2Sb_2Te_5$ the re-crystallization is substantially faster than the crystallization of as deposited material which is the typical behavior.

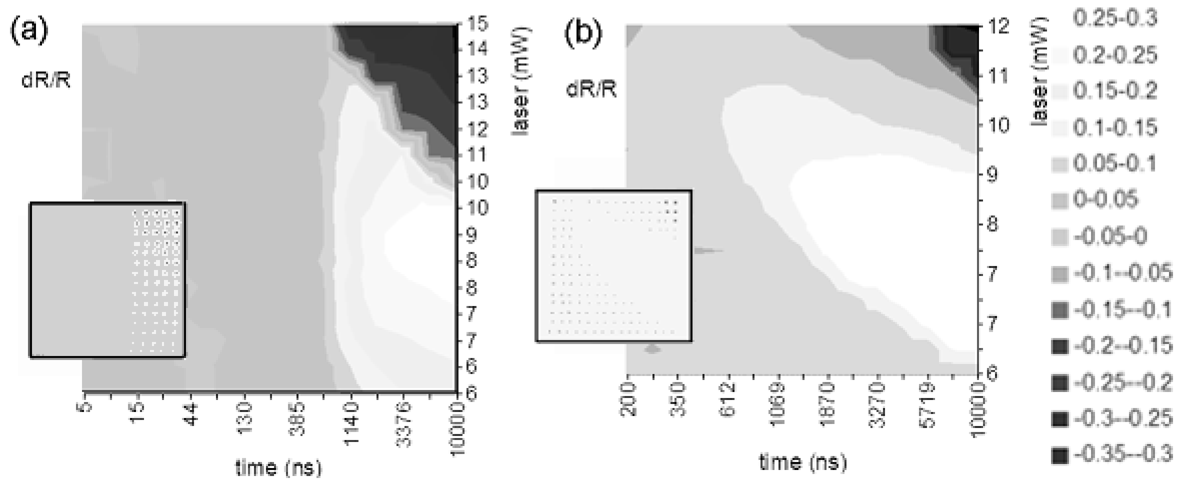

Fig. 7: (a) Single pulse experiment on as-deposited, amorphous $Ge_3Sb_6Te_5$ film. Insert: Optical microscope image. (b) Pre-pulse experiment on crystalline $Ge_3Sb_6Te_5$ (50 ns, 30 mW pre-pulse). Insert: Optical microscope image.

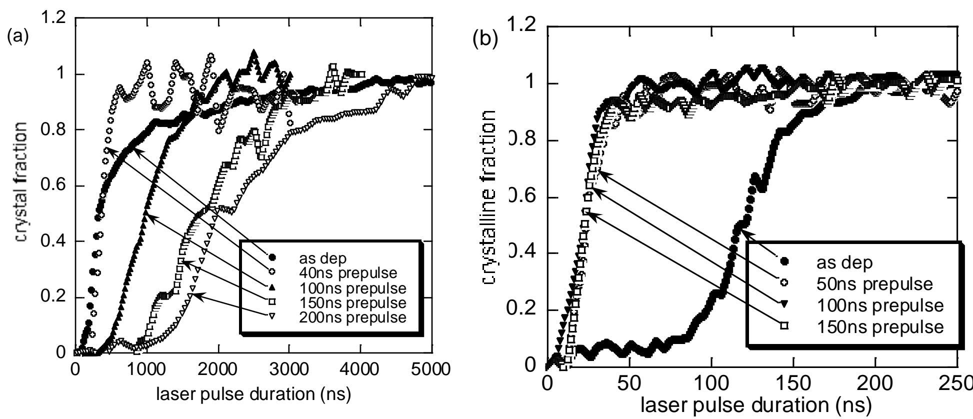

Fig. 8: (a) Crystal fraction as a function of laser duration for as deposited $Ge_3Sb_6Te_5$ compared to pre-pulse (re-crystallization) experiments with variable pre-pulse length on crystalline material. (b) The same for $Ge_2Sb_2Te_5$.

The re-crystallization time for $Ge_3Sb_6Te_5$ depends on the size of the melt-quenched mark (growth-dominated) while it does not for $Ge_2Sb_2Te_5$ (nucleation-dominated). From the sizes of the melt-quenched marks measured by AFM (500 - 1400 nm for 40 – 200 ns, 30 mW pulses) and the re-crystallization times as a function of pre-pulse duration (Fig. 8a) a crystal growth speed was estimated again, it was between 0.2 and 0.6 m/s. Figure 9 shows an AFM image of two laser spots in the crystalline $Ge_3Sb_6Te_5$ that were first melt-quenched and then attempted to re-crystallize.

Fig. 9: AFM images of laser spots in crystalline $Ge_3Sb_6Te_5$ that were first melt-quenched and then attempted to re-crystallize.

These dots were not fully re-crystallized, one can see the outer region of the dots that have been re-crystallized, but the middle is still amorphous. It is nicely visible that the crystal growth happens from the edge of the spot towards the middle, this confirms the growth-dominated character of this material.

Interestingly, even though $Ge_3Sb_6Te_5$ shows the re-crystallization behavior of a growth-dominated material, it does not show the two different types of crystallization for the as deposited material that was observed in $Ge_{15}Sb_{85}$ and AIST, namely reproducible crystallization at low powers, and more random behavior at higher power. An increase in the incubation time was observed for powers higher than 5 mW, but at 6-7 mW ablation started which might have obscured the random crystallization. Studies should be performed on a more thermally conducting substrate to investigate this point. $Ge_2Sb_2Te_5$ shows very fast re-crystallization in about 30 ns, one reason why this material has been so successful in both optical and PCRAM applications.

4. CONCLUSION

Various phase change materials were studied and their crystallization times measured using static laser testers. For most materials studied here the re-crystallization time of melt-quenched, amorphous material is shorter than the crystallization time of as-deposited, amorphous material. The largest difference was found for the growth-dominated $Ge_{15}Sb_{85}$, almost three orders of magnitude (20 ns vs. 5 μs), but also nucleation-dominated $Ge_2Sb_2Te_5$ shows a large difference (30 ns vs. 150 ns). It was demonstrated that the crystallization time depends on numerous factors such as substrate and laser power (which translates into maximum temperature). The evaluation of the switching time of a phase change material for technological applications should be performed under conditions which are as close as possible to the actual device or disc conditions because so many factors influence it substantially. The crystallization time of as-deposited films can be very misleading if it is used to evaluate the material for technological applications.

REFERENCES

1. S. R. Ovshinsky, Phys. Rev. B **21** (1968) 1450
2. N. Yamada, E. Ohno, K. Nishiuchi, N. Akahira, and M. Takao, J. Appl. Phys. **69** (1991) 2849
3. B.-S. Lee, S. Raoux, R. Shelby, C. T. Rettner, G. W. Burr, S. Bogle, S. G. Bishop, J. R. and Abelson, Europ. Phase Change and Ovonic Sci. Symp., Zermatt, Switzerland, September 2007
4. N. Ohshima, J. Appl. Phys. 79 (1996) 8357
5. G.-F. Zhou, Mater. Sci. Engin. **A304-306** (2001) 73
6. H. C. F. Martens, R. Vlutters and J. C. Prangsma, J. Appl. Phys. **95** (2004) 3977
7. X. Wei, L. Shi, T. C. Chong, R. Zhao and H. K. Lee, Jpn. J. Appl. Phys. **46** (2007) 2211
8. V. Weidenhof, I. Friedrich, S. Ziegler and M. Wuttig, J. Appl. Phys. **86** (1999) 5879
9. M. Salinga, PhD thesis, Technical University Aachen, Germany
10. S. Raoux, Charles T. Rettner, J. L. Jordan-Sweet, A. J. Kellock, T. Topuria, P. M. Rice, and D. C. Miller, J. Appl. Phys. **102** (2007) 94305
11. M. Wuttig and N. Yamada, Nature Mater. **6** (2007) 824
12. J. Kalb, F. Spaepen and M. Wuttig, J. Appl. Phys. **98** (2005) 054910
13. www.comsol.com
14. Y.-C. Chen, C. T. Rettner, S. Raoux, G. W. Burr, S. H. Chen, R. M. Shelby, M. Salinga, W. P. Risk, T. D. Happ, G. M. McCleland, M. Breitwisch, A. Schrott, J. B. Philipp, M. H. Lee, R. Cheek, T. Nirschl, M. Lamorey, C. F. Chen, E. Joseph, S. Zaidi, B. Yee, H.-L. Lung, R. Bergmann and C. Lam, IEDM Tech. Dig., 777-780 (2006)
15. J. Kalb, F. Spaepen and M. Wuttig, Appl. Phys. Lett. **84** (2004) 5240
16. I Friedrich, V. Weidenhof, W. Njoroge, P. Franz and M. Wuttig. J. Appl. Phys. **87** (2000) 4130